JOURNAL OF BIOMOLECULAR STRUCTURE AND DYNAMICS
https://doi.org/10.1080/07391102.2021.1889665

Taylor & Francis
Taylor & Francis Group

A potential peptide inhibitor of SARS-CoV-2 S and human ACE2 complex

Grijesh Jaiswal, Shivani Yaduvanshi and Veerendra Kumar

Amity Institute of Molecular Medicine and Stem Cell Research (AIMMSCR), Amity University, Noida, India

Communicated by Ramaswamy H. Sarma

ABSTRACT

The disease COVID-19 has caused heavy socio-economic burden and there is immediate need to control it. The disease is caused by severe acute respiratory syndrome coronavirus 2 (SARS-CoV-2) virus. The viral entry into human cell depends on the attachment of spike (S) protein *via* its receptor binding domain (RBD) to human cell receptor angiotensin-converting enzyme 2 (hACE2). Thus, blocking the virus attachment to hACE2 could serve as potential therapeutics for viral infection. We have designed a peptide inhibitor (ΔABP-α2) targeting the RBD of S protein using *in-silico* approach. Docking studies and computed affinities suggested that peptide inhibitor binds at the RBD with ∼95-fold higher affinity than hACE2. Molecular dynamics (MD) simulation confirms the stable binding of inhibitor to hACE2. Immunoinformatics studies suggest non-immunogenic and non-toxic nature of peptide. Thus, the proposed peptide could serve as potential blocker for viral attachment.

ARTICLE HISTORY
Received 14 October 2020
Accepted 5 February 2021

KEYWORDS
SARS-CoV-2; COVID-19; peptide inhibitor; immunoinformatics; receptor binding domain; spike S protein; angiotensin-converting enzyme 2 (ACE2)

Introduction

The ongoing global pandemic COVID-19 is caused by a novel β-coronavirus severe acute respiratory syndrome coronavirus 2 (SARS-CoV-2) (previously known as 2019-nCoV). The virus was first reported in the Wuhan (China) where it caused an outbreak of pulmonary disease in late December 2019 (Wu, Zhao, et al., 2020; Zhou, Yang, et al., 2020). SARS-CoV-2 is the third coronavirus to cause influenza like illness after SARS-CoV and MERS-CoV. It transfers from human to human efficiently. Coronaviruses are positive-sense single-stranded RNA virus enveloped with nucleocapsid of helical symmetry (Spaan et al., 1988). SARS-CoV-2 genome is about 82% identical to the SARS-CoV (Ren et al., 2020; Zhu et al., 2020).

The S protein extensively decorates the virion surface as crown (therefore, called corona). The spike (S) protein is a type I membrane protein and is glycosylated at 22 sites (Kumar et al., 2020; Simmons et al., 2004; Walls et al., 2016, 2020). N-glycans linked to N165 and N234 stabilise the RBD 'up' conformation and favours S protein binding to hACE2 (Casalino et al., 2020). The S protein is analogous to influenza hemagglutinin (HA), respiratory syncytial virus (RSV) fusion glycoprotein (F) and human immunodeficiency virus (HIV) gp160 (Env). It facilitates the coronavirus entry into host cell (Li, 2016; Wan et al., 2020). The S protein consists of receptor binding S1 and membrane fusion S2 subunits. The S1 subunit consists of a receptor-binding domain (RBD) and a core domain. The RBD consists of a receptor-binding motif (RBM), which interacts with the claw-like structure of hACE2 (F. Li et al., 2005; W. Li et al., 2004). The S1 adopts an elongated structure and undergoes transient hinge-like motions to become either receptor accessible or inaccessible. The monomeric form consists of a large ectodomain, a single-pass transmembrane anchor and a short intracellular tail at C-terminus (Bosch et al., 2003; Gao et al., 2013).

The virus entry to human cell starts with the attachment of S protein to the cell membrane protein receptor angiotensin-converting enzyme 2 (ACE2) (W. Li et al., 2003; Tai et al., 2020). The human ACE2 (hACE2) is expressed on the surface of alveolar cells in the lungs. Upon binding to hACE2, the S protein is cleaved to S1 and S2 subunits at furin-like cleavage site (Coutard et al., 2020; Hoffmann et al., 2020; Xia et al., 2020). The RBD through its RBM site directly binds to the peptidase domain (PD) of hACE2 (Shang et al., 2020; Yan et al., 2020). Later, S1 subunit dissociates from hACE2 and S2 subunit adopts a post fusion state for membrane fusion (Coutard et al., 2020; Shang et al., 2020; Yan et al., 2020). The viral membrane and host cell membrane fuse to form a pore and then viral genome is injected into the host cell. This leads to the COVID-19 disease, which is associated with a major immune inflammatory response. Temperature dependent Molecular dynamics (MD) simulation suggests that RBM motif begins to close at 40 °C and closes completely at 50 °C. In close conformation receptor binding residues are hidden and hACE2 cannot bind (Rath & Kumar, 2020). Deaths are due to respiratory failure associated with cytokine storm with high serum levels of pro-inflammatory cytokines and chemokines (Feldmann et al., 2020).

SARS-CoV-2 spike (S) protein binds to hACE2 with higher affinity than the other SARS-CoV S proteins, a likely reason for high infectivity of SARS-CoV-2 (Lan et al., 2020; Walls et al., 2020; Wrapp et al., 2020). The monoclonal antibodies

CONTACT Veerendra Kumar vkumar34@amity.edu Amity Institute of Molecular Medicine and Stem Cell Research (AIMMSCR), Amity University, Noida, Uttar Pradesh 201303, India.

Supplemental data for this article can be accessed online at https://doi.org/10.1080/07391102.2021.1889665.

for SARS-CoV S protein are not able to neutralise SARS-CoV-2 (Tian et al., 2020). Thus, despite the high sequence and structural similarity, there are notable differences between the SARS-CoV and SARS-CoV-2 S proteins. Further, MD simulation studies suggested a stable salt bridge between Lys417/Asp30 (SARS-CoV-2/hACE2) and three stable hydrogen bonds between Tyr449/Asp38, Gln493/Glu35 and Gln498/Lys353 (SARS-CoV-2/hACE2) in SARS-CoV-2/hACE2 complex but not in SARS-CoV/hACE2 (Ali & Vijayan, 2020). The affinity between the viral RBD and host ACE2 during the initial attachment of virus determines the susceptibility of hosts to the SARS-CoV infection (Belouzard et al., 2012; F. Li, 2015; W. Li et al., 2004). Thus, viral entry into the host cell is a critical step in viral infection and could be exploited for therapeutics development.

The current pandemic has created immediate needs for therapeutics to treat COVID-19. Computational approaches have been employed to discover the potential drugs against SARS-CoV-2 (Chandel et al., 2020; Khan et al., 2020; Mirza & Froeyen, 2020; Wu, Liu, et al., 2020; Zhou, Hou, et al., 2020). Drugs targeting either the S protein or the protease domain, have been screened. The inhibitors that can effectively block association of the SARS-CoV-2 S protein with hACE2 may have the potential to treat COVID-19. In our previous study, we have identified a double helical inhibitor amantadine binding protein (ΔABP)-D25Y (residue 65) that binds at the RBM site of SARS-CoV-2 RBD with higher affinity than hACE2. Here, we reported that the helix 2 of ΔABP-D25Y (called ΔABP-α2) alone is highly effective to block the association of SARS-CoV-2 RBD/hACE2.

Materials and methods

Structural analysis

All the protein structures were downloaded from Protein Data Bank (PDB) and their codes are mentioned as they appear in the manuscript (Berman et al., 2000). The structures were manually visualised and manipulated in Coot, Pymol and UCSF Chimera (DeLano, 2002; Emsley et al., 2010; Pettersen et al., 2004). Structural comparison was done using Pymol. All the figures were prepared using Pymol (DeLano, 2002). Binding affinities were computed using the PRODIGY server. The program computes the interfacial contacts and non-interacting surface in a protein complex (Xue et al., 2016).

Molecular docking

Molecular docking is used to dock the binding of a peptide or ligand on a macromolecule. The RBD domain (336-518) of SARS-CoV-2 S protein (PDB 6M17) was used as a receptor. The ΔABP-α1 (LKYLVKQLERALRELKKSLDELERSLEELEKN), ΔABP-α1-V10K (LKYLKKQLERALRELKKSLDELERSLEELEKN), ΔABP-α1-D25Y (LKYLVKQLERALRELKKSLYELERSLEELEKN), ΔABP-α1-V10K-D25Y (LKYLKKQLERALRELKKSLYELERSLEELEKN), and ΔABP-α2 (PSEDALVENNRLNVENNKIIVEVLRIIL) peptides were docked using HADDOCK2.4 program (van Zundert et al., 2016). Mutations in peptide sequences are underlined. Docking by HADDOCK program is driven by prediction of likely residues (called ambiguous interaction restraints [AIRs]) found at the interface. These residues may be active (interacting residue) or passive (nearby interacting residue). The binding interface of RBD and peptides were predicted using CPORT (de Vries & Bonvin, 2011) and BIPSPI (Sanchez-Garcia et al., 2019) servers as described previously (Jaiswal & Kumar, 2020). Before docking protocol, the pdbs were 'cleaned' by removing water and non-bonded ions in a text editor. The HADDOCK program has generated about 200 complexes and clustered them. The cluster with highest HADDOCK score and lowest electrostatic energy was selected. The best complex was chosen based on cluster size, HADDOCK score and electrostatic energy.

Molecular dynamics (MD) simulation

The MD simulation was performed for RBD/ΔABP-α2 complex in Gromacs 2020.2 for 100 ns (Abraham et al., 2015). Simulation inputs were built using CHARMM-GUI web with CHARMM36 force field (Jo et al., 2008; Lee et al., 2016). The complex was immersed in a cubic box filled with TIP3P water molecules and 150 mM NaCl. Sodium and chloride ions were added to neutralise the charge of the system. MD simulation was run using periodic boundary conditions (PBC). Initial geometries of the system were minimised with 5000 steps with the steepest descent algorithm. The system was relaxed at 303 K and 1 atm for 500 ps at 2 fs time steps. Production MD was performed for 100 ns. During production run temperature was maintained at 303 K using velocity rescaling. Bond lengths were constrained with the LINCS algorithm. The pressure was controlled by isotropic coupling using Parrinello-Rahman barostat. A Verlet scheme was used for van der Waals and Particle Mesh Ewald electrostatics interactions within 1.2 nm. Van der Waals interactions were switched above 1.0 nm.

Principal component analysis (PCA)

Principal component analysis (PCA) was done to detect the direction and amplitude of the dominant motions in the MD trajectory (Yang et al., 2009). PCA method is used to reduce the complexity of a data set to extract biologically relevant movements of protein domains. GROMACS in built tool covar was used to obtain eigenvalues and eigenvectors by calculating and diagonalising the covariance matrix. This removed the translational and rotational components from the system. The eigenvectors that correspond to the largest eigenvalues are called principal components (PCs). They represent the largest-amplitude collective motions. GROMACS utility tool anaeig was used to analyse the eigenvectors.

Immunoinformatics

To predict the drug ability of peptide ΔABP-α2, immunogenic and toxic properties were determined using various

Table 1. HADDOCK docking statistics of various ΔABP peptides.

Peptides	HADDOCK score[a]	Van der Waals energy (E_{vdw}) (kcal mol^{-1})	Electrostatic energy (E_{elec}) (kcal mol^{-1})	Desolvation energy (E_{desol}) (kcal mol^{-1})	Restraints violation energy (E_{AIR}) (kcal mol^{-1})	PRODIGY dissociation constant nM (ΔG kcal mol^{-1})
ΔABP-α1	−68.7 ± 5.0	−53.7 ± 4.5	−217.4 ± 26.4	−2.3 ± 2.4	308.1 ± 20.08	2.6 (−11.7)
ΔABP-α1-V10K	−71.7 ± 8.6	−51.0 ± 2.1	−236.7 ± 30.2	−2.0 ± 0.6	286.8 ± 67.00	16.0 (−10.6)
ΔABP-α1-D25Y	−70.6 ± 3.8	−61.5 ± 5.0	−127.5 ± 42.2	−16.8 ± 3.1	331.9 ± 72.20	5.2 (−11.3)
ΔABP-α1-V10K-D25Y	−66.0 ± 4.9	−49.8 ± 5.8	−161.6 ± 31.5	−19.2 ± 5.2	353.2 ± 62.52	69.0 (−12.6)
ΔABP-α2	−74.0 ± 5.3	−54.9 ± 5.3	−200.6 ± 15.1	−10.0 ± 3.8	310.2 ± 64.25	0.049(−14.1)

[a]HADDOCK score: 1.0 E_{vdw} + 0.2 E_{elec} + 1.0 E_{desol} + 0.1 E_{AIR}.

immunoinformatic tools. The peptide sequence of the ΔABP-α2 was used for different immunoinformatic studies. The protective antigens were predicted from VaxiJen 2.0 with default parameters (Doytchinova & Flower, 2007). The server uses bacterial, viral and tumour protein datasets. It outputs the antigenicity score using the physicochemical properties of the proteins.

The T-cell epitopes were identified using NetCTL version 1.2 server which outputs the combinatorial score of MHC-I binding, proteasomal C-terminal cleavage and TAP transport (Larsen et al., 2007). The B cell epitope prediction was done using IEDB tool. DiscoTope tool was used to predict the conformational B cell epitope (Kringelum et al., 2012). To check if the peptide is toxic and can cause damage to the cell, ToxinPred server was used (Gupta et al., 2013). The server allows to predict the toxicity of peptides shorter than 50 amino acids.

Results

Several SARS-CoV-2 RBD/hACE2 complex structures have been solved and deposited in PDB. We used pdb 6M17 for our analysis. The peptide inhibitor is derived from ABP (pdb code 6H9H) as described in our previous study (Jaiswal & Kumar, 2020). In brief, we have reported a double helical protein ABP (pdb 6n9h) structurally homologous to the PD domain of hACE2. ABP is a synthetic peptide (80 AA) and is known for binding to the drug amantadine, hence called ABP. Removing few residues from both N- and C-terminus (ΔABP, 65 AA) and a point mutation D25Y (ΔABP-D25Y) greatly improves the affinity to SARS-CoV-2 RBD. MD simulation study has confirmed the stable binding of ΔABP-D25Y to SARS-CoV-2 RBD. Thus, ΔABP-D25Y could serve as potential blocker of viral S and hACE2 (Jaiswal & Kumar, 2020). In this study, we have analysed the individual helices of ΔABP.

Docking analysis

The previously identified inhibitor (ΔABP-D25Y) of RBD has two helices (α1 and α2) homologous to the PD domain of hACE2 (Jaiswal & Kumar, 2020). The inhibitor (ΔABP-D25Y) binds to RBD with higher affinity compared to hACE2. To further examine, the role of individual helices of ΔABP in interaction with RBD, we examined the following peptides – ΔABP-α1, ΔABP-α2, ΔABP-α1-V10K, ΔABP-α1-D25Y and ΔABP-α1-V10K-D25Y. The mutations (D25Y and V10K) were introduced to complement the α1 helix of hACE2 (Jaiswal & Kumar, 2020). We docked all peptides into SARS-CoV-2 RBD. The interaction restraints were generated using CPORT and BIPSPI servers (de Vries & Bonvin, 2011; Sanchez-Garcia et al., 2019). Both servers predicted peptides binding at RBM site of RBD. Therefore, RBM site residues (483–507) and all residues of peptides were used as active residues for docking. Best complex structures were selected based on the cluster size and the HADDOCK score. HADDOCK score is computed as a weighted sum of van de waals, electrostatic, desolvation and AIRs energies. The ΔABP-α2 showed the best HADDOCK score (Table 1). ΔABP-α2 peptide sits between the two helices of ΔABP-D25Y (Figure 1(A) and Supplementary file 1). The N terminus and C-terminus of peptide are shifted about 8.9 and 3.2 Å respectively, towards RBD in comparison to α2/ΔABP-D25Y. Thus, the ΔABP-α2 is closer to RBD compared to ΔABP-D25Y. The ΔABP-α2 peptide partially overlaps with α1/hACE2 (Figure 1(B)). The fragment up to residue Ile56 (His34 of hACE2) superimpose very well. From residue Glu35 (hACE2) onwards the α1/hACE2 deviates away from SARS-CoV-2 RBD. However, ΔABP-α2 peptide lies parallel to RBM throughout its length (Figure 1(B)). Hence the bound peptide showed higher binding contacts with SARS-CoV-2 RBD (Table 2).

However, the ΔABP-α1 peptide and its mutants bind SARS-CoV-2 RBD with lower affinity (Table 1). Further, the ΔABP-α1 peptides bind at a different position than α1/ΔABP-D25Y (Supplementary Figure 1(A)). The ΔABP-α2 peptide also binds RBD of other coronaviruses at the same site. Binding score varies depending on the RBM site residues. The ΔABP-α2 peptide binds 2005–2006 SARS coronavirus civet strain RBD (pdb 3d0i) with best HADDOCK score (−85.6 ± 0.2). The binding score is better than SARS-CoV-2 RBD. However, the bound peptide does not cover the whole RBM site (Supplementary Figure 1(B)). Thus, the proposed inhibitor has the potential to block the broader range of coronaviruses.

Binding affinity

The binding affinity of therapeutic agents to the receptor is an important parameter in predicting their effectiveness as promising drug candidates. To compute the binding affinity of peptides, we use PRODIGY server. The binding affinities of individual peptides are listed in Table 1. The predicted affinities are in accordance with HADDOCK score. The PRODIGY server predicted a dissociation constant (K_D) of 2.6 nM (ΔG −11.7 kcal mol^{-1}) and 0.049 nM (ΔG −14.1 kcal mol^{-1}) for ΔABP-α1 and ΔABP-α2 peptides, respectively. The predicted K_D of ΔABP-D25Y is 0.6 nM (ΔG −12.6 kcal mol^{-1}) (Jaiswal &

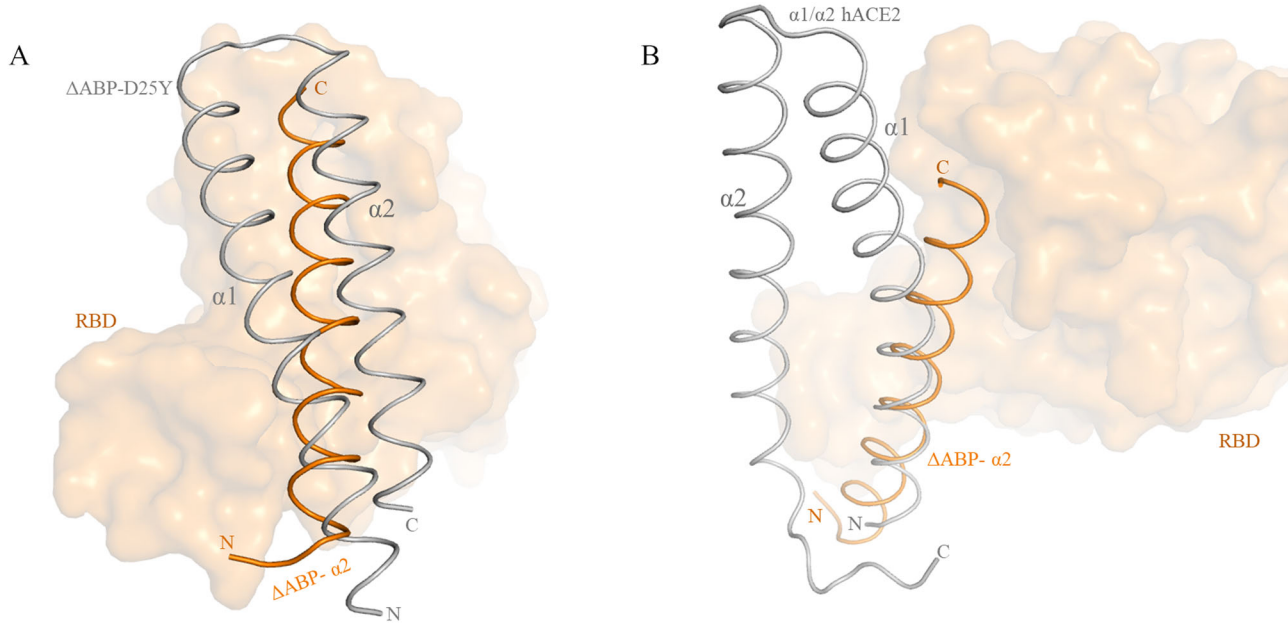

Figure 1. Binding of peptide inhibitor ΔABP-α2 on the SARS-CoV-2 RBD. (A) The peptide inhibitor ΔABP-α2 binds on RBD at a site which is between the two helices of ΔABP-D25Y binds. The receptor-binding domain (RBD) is shown as surface. (B) The Peptide inhibitor ΔABP-α2 binding partially overlaps with the α1/hACE2. The ΔABP-α2 inhibitor showed much higher affinity for hACE2 because it forms more interaction with hACE2.

Table 2. MM-GBSA binding energy calculation of RBM site and ΔABP-α2 peptide residues.

RESIDUE	VDW	ELE	GB	SA	Total	RESIDUE	VDW	ELE	GB	SA	Total
		RBM Site						ΔABP-α2			
RBD/ΔABP-α2	−93.14	−189.56	232.76	−13.36	−63.31						
G-476	−0.83	1.11	−0.07	−0.13	0.08	P-38	−1.83	2.5	0.29	−0.44	0.52
S-477	−1.83	−7.05	7.35	−0.44	−1.96	S-39	−0.74	−0.42	0.41	−0.1	−0.85
T-478	−0.94	−0.11	0.54	−0.16	−0.67	E-40	−0.09	−10.09	10.04	0	−0.14
P-479	−0.11	−0.25	0.26	−0.01	−0.12	D-41	−0.29	−14.7	15.28	−0.01	0.27
C-480	−0.03	−0.31	0.37	0	0.03	A-42	−1.77	0.65	0.47	−0.32	−0.98
N-481	−0.01	0.03	0.01	0	0.03	L-43	−1.15	−0.6	0.58	−0.25	−1.41
G-482	−0.01	−0.19	0.23	0	0.04	V-44	−0.15	−0.03	0.13	0	−0.05
E-484	−0.1	15.54	−14.98	0	0.46	E-45	−1.05	−20.57	21.41	−0.06	−0.27
G-485	−0.09	1.17	−0.87	0	0.21	N-46	−4.82	−1.78	4.84	−0.65	−2.41
F-486	−2.51	−0.81	1.94	−0.57	−1.95	N-47	−0.67	−0.1	0.86	−0.13	−0.04
N-487	−2.49	−3.1	5.15	−0.29	−0.73	R-48	−0.45	22.35	−21.15	−0.02	0.74
C-488	−0.51	0.54	−0.35	0	−0.32	L-49	−3.29	−1.31	1.74	−0.57	−3.44
Y-489	−3.52	−1.86	2.54	−0.59	−3.43	N-50	−1.89	0.75	0.96	−0.23	−0.41
F-490	−0.24	0.06	0.37	0	0.19	V-51	−0.19	0.23	−0.07	0	−0.03
P-491	−0.13	0.56	−0.56	0	−0.13	E-52	−1.85	−48.67	49.25	−0.36	−1.64
L-492	−0.13	−0.07	0.33	0	0.14	N-53	−3.1	−2.5	3.71	−0.55	−2.43
Q-493	−2.11	−3.3	4.94	−0.39	−0.86	N-54	−0.24	0.16	0.27	0	0.18
S-494	−0.94	0.88	0.82	−0.13	0.64	K-55	−0.42	32.39	−30.92	−0.02	1.03
Y-495	−1.81	0.85	0.82	−0.22	−0.35	I-56	−3.15	0.09	0.11	−0.5	−3.44
G-496	−1.51	2.02	−0.75	−0.14	−0.38	I-57	−0.72	−0.84	0.87	−0.1	−0.78
F-497	−1.45	−1.79	1.9	−0.07	−1.41	V-58	−0.17	0.24	0.01	0	0.08
Q-498	−2.9	2.32	−1.16	−0.31	−2.03	E-59	−0.34	−45.42	43.31	−0.28	−2.72
P-499	−0.24	−0.92	1.12	0	−0.03	V-60	−2.8	−0.67	0.75	−0.41	−3.14
T-500	−0.45	−12.57	8.71	−0.25	−4.55	L-61	−0.4	−0.07	0.34	0	−0.12
N-501	−2.65	−2.42	4.85	−0.41	−0.63	R-62	−2.3	23.66	−20.3	−0.4	0.65
G-502	−0.11	1.79	−1.81	0	−0.13	I-63	−7.25	−1.15	2.5	−1.07	−6.97
V-503	−0.04	0.45	−0.41	0	0	I-64	−4.35	0.36	1.09	−0.69	−3.58
G-504	−0.07	−0.1	0.26	0	0.09	L-65	−1.11	−29.24	32.09	−0.32	1.41
Y-505	−2.7	−1.58	2.44	−0.35	−2.19						
Q-506	−0.27	−2.27	2.41	0	−0.14						
P-507	−0.14	−0.14	0.11	0	−0.18						

VDW: Van der Waals potentials, ELE: electrostatic potentials, GB: polar solvation free energies predicted by the Generalised Born model, SA: nonpolar contribution to the solvation free energy calculated by an empirical model.

Kumar, 2020). The dissociation constants of mutant ΔABP-α1-V10K, ΔABP-α1-D25Y and ΔABP-α1-V10K-D25Y are 16.0 nM (ΔG −10.6 kcal mol^{-1}), 5.2 nM (ΔG −11.3 kcal mol^{-1}) and 69 nM (ΔG −9.8 kcal mol^{-1}), respectively. The order of peptides affinity to SARs-CoV-2 RBD is ΔABP-α2 > ΔABP-α1 > ΔABP-D25Y> ΔABP-α1-D25Y > ΔABP-α1-V10K > ΔABP-α1-V10K-D25Y. The experimentally determined K_D for hACE2 to ectodomain S protein interaction is 4.7 nM (Lan et al.,

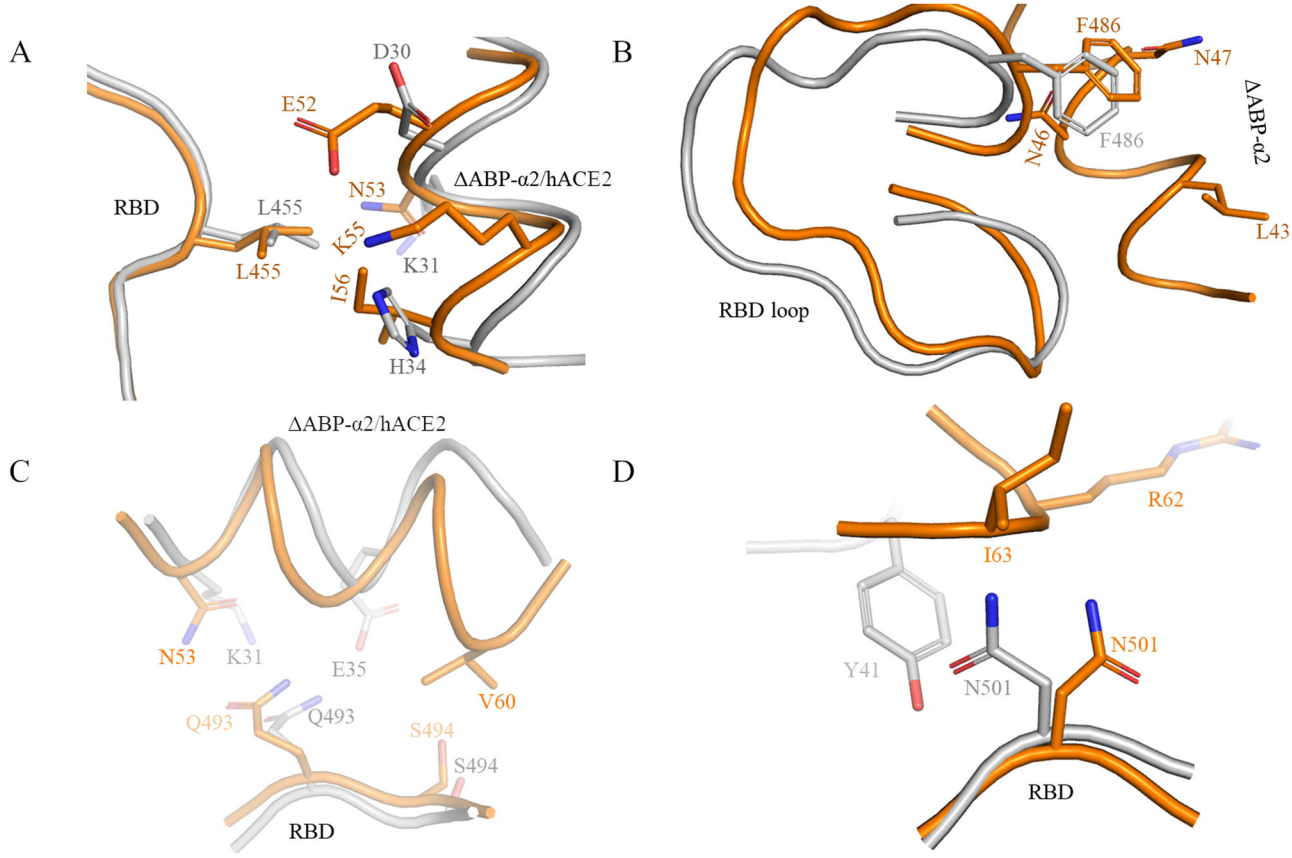

Figure 2. Interaction of viral RBD and ΔABP-α2 peptide. All critical amino acid residues (A) Leu455, (B) Phe486, (C) Gln493, Ser494 and (D) Asn501 are involved in the interaction with ΔABP-α2 peptide. The SARS-CoV-2 RBD/ΔABP-α2 complex is shown in orange and SARS-CoV-2 RBD/hACE2 complex is shown in grey.

2020; Walls et al., 2020). Thus, ΔABP- α2 peptide binds SARS-CoV-2 RBD with higher affinity (∼95 fold) than hACE2. A designed inhibitor should have a selective binding at the target site with relatively high binding energies. Thus, HADDOCK score and predicted K_D suggests that ΔABP-α2 peptide binds RBD with remarkably high affinity.

RBD/ΔABP-α2 complex

The peptide ΔABP-α2 is parallelly aligned with RBM β sheet and covers the RBM site fully (Figure 1). The N-terminus of peptide interacts with the RBD capping loop (472–488) and C-terminus of peptide interacts with RBD loop (498–505). Thus, ΔABP-α2 peptide forms extensive contact with SARS-CoV-2 RBD. Sequence analysis of coronaviruses RBDs suggests that SARS-CoV-2 RBD has unique residues- Leu455, Phe486, Gln493, Ser494 and Asn501. These unique residues form extensive contact with the hACE2 and responsible for higher affinity of SARS-CoV-2 RBD to hACE2 (Shang et al., 2020; Yan et al., 2020). Thus, the designed inhibitor should disengage these residues from hACE2 interaction.

Leu455 of SARS-CoV-2 RBD enhances the viral binding to hACE2 because of its favourable interactions with hotspot 31 (Lys31 of hACE2) (Wan et al., 2020). In SARS-CoV-2 RBD, Leu455 interacts with Asp30, Lys31 and His34 of hACE2. In RBD/ΔABP-α2 peptide complex, Leu455 interacts with Glu52, Asn53, Lys55 and Ile56 (Figure 2(A)). In SARS-CoV-2 RBD, Phe486 does not interact with α1/hACE2. Capping loop which harbours Phe486 is flexible and deviates towards bound peptide in ΔABP-α2 complex. In RBD/ΔABP-α2 complex, the Phe486 is coordinated by triad Leu43, Asn46 and Asn47. The phenyl ring of Phe486 is sandwiched between side chain of Asn46 and Asn47 (Figure 2(B)). In SARS-CoV-2 RBD, Gln493 forms salt bridge interactions with Lys31 and Glu35 of hACE2. In RBD/ΔABP-α2 complex also, Gln493 forms similar strong salt bridge interaction with Asn53 of peptide (Figure 2(C)). Ser494 does not form any contact with hACE2 in SARS-CoV-2 RBD/hACE2 complex. However, in RBD/ΔABP-α2 complex Ser494 forms interaction with Val60 of ΔABP-α2 enhancing peptide interaction with viral RBD (Figure 2(C)). Lastly, Asn501 in SARS-CoV-2 RBD/hACE2 complex interacts with Tyr41 of ACE2. However, Asn501 interacts with Arg62 and Ile63 of peptide in RBD/ΔABP-α2 complex (Figure 2(D)). Thus, ΔABP-α2 can form very strong interaction with RBD.

We further calculated the binding affinity for the RBD/ΔABP-α2 complex using MM-GBSA method on HawkDock server (Weng et al., 2019). The total binding energy of the ΔABP-α2 and RBD is −63.31/kcal/mol (Table 2). The binding energy contribution of individual residues confirms that unique RBD residues of SARS-CoV-2 forms strong interaction with ΔABP-α2 (Table 2). The van de waals and electrostatic energies calculated from HADDOCK and MM-GBSA are in good agreement (Tables 1 and 2).

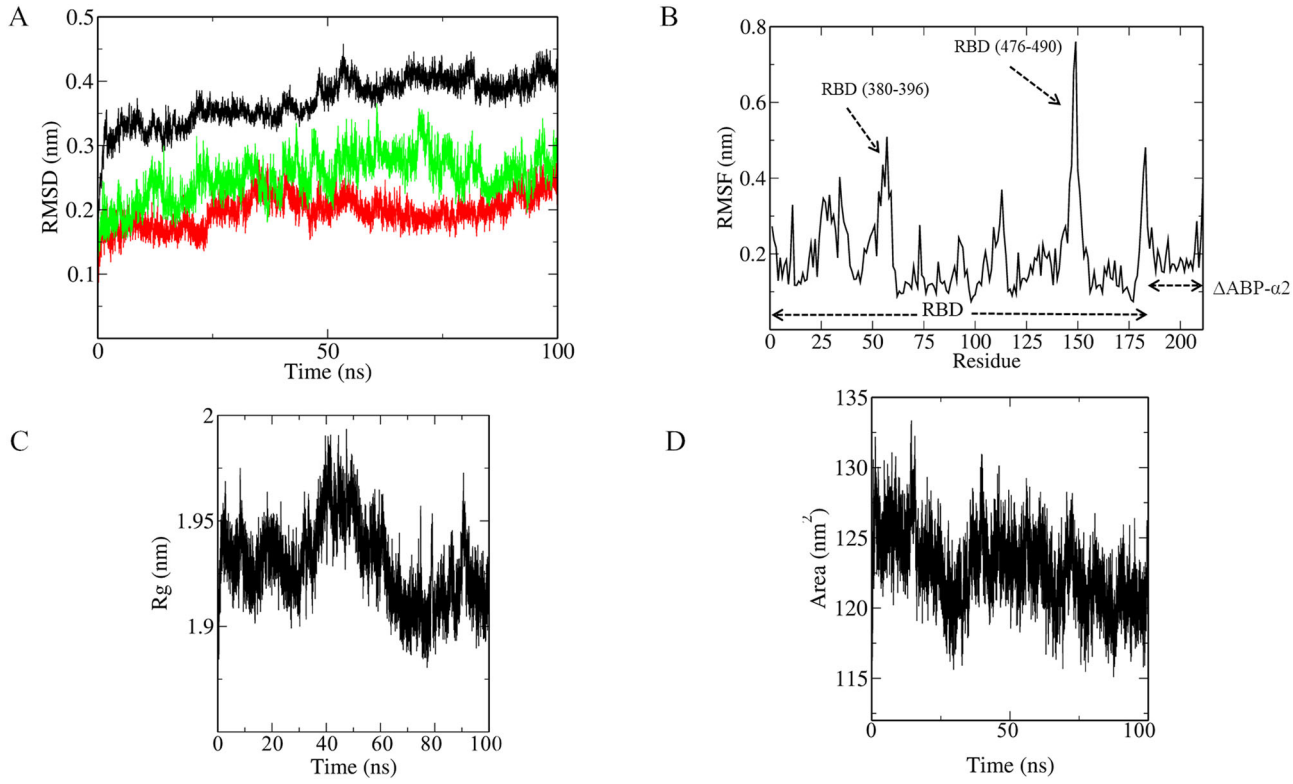

Figure 3. MD simulation of SARS-CoV-2 RBD/ΔABP-α2 complex. (A) RMSD analysis of MD simulation trajectory of whole complex (black), peptide inhibitor (green) and RBM site (red). (B) Averaged root-mean-square fluctuation for each amino acid in SARS-CoV-2 RBD/ΔABP-α2 complex. RBD and ΔABP-α2 peptide residues are shown by dotted arrow. (C) Radius of gyration (Rg) of the complex during the 100 ns simulation. (D) Solvent accessible surface area (SASA) is shown during simulation.

MD Simulation

The MD simulation calculates the time dependent behaviour of the molecular system. Advent of high-performance computing (HPC) and simplification of MD algorithms have made possible to simulate the entire proteins in solution, membrane embedded proteins or large macromolecular complexes like nucleosomes or ribosomes (Brandman et al., 2012; Roccatano et al., 2007; Sharma et al., 2007; Tinoco & der, 2009). The fluctuations and conformational changes of biological macromolecules can be studied using MD simulations. Conformational ensembles of a molecule can also be analysed using MD simulations at biologically relevant time scale. To understand the interactions between viral RBD and ΔABP-α2, 100 ns classical MD simulation of the complex was performed. To assess the dynamic behaviour of the complex, the time dependent root-mean-square deviation (RMSD) of all protein atoms was calculated using original docked complex as reference. The RMSD value of the whole complex fluctuates between 0.3-0.4 nm suggesting flexible nature of the complex (Figure 3(A)). However, the RBM site and ΔABP-α2 peptide exhibit RMSD value of ∼0.2 nm. Thus, the interface between peptide inhibitor and RBM is quite stable (Figure 3(A)).

The dynamic behaviour of the protein at residue level was estimated by RMS fluctuations (RMSF). RMSF reflects the positions of the individual atoms with respect to the average position across the whole simulation trajectory. The peptide ΔABP-α2 residues are rigid and do not fluctuate much (RMSF $<$ 0.15 nm) (Figure 3(B)). Similarly, the RBD residues are stable except some the loops. Particularly two flexible regions are present in the RBD. The loop (380–396) on the RBD surface is flexible. This loop is far from the ΔABP-α2 interaction site. The second flexible region is the capping loop (476–490) near the ΔABP-α2 interaction site. The composition of this loop is remarkably different from SARS-COV. The following mutations Pro469/Val483, Pro470/Glu484, Thr468/Gly482, Cys467/Cys480, Lys465/Thr478, Asp463/Gly476 and Pro462/Ala475 (SARS-CoV/SARS-CoV-2) make SARS-CoV-2 loop more flexible. Additionally, an extra amino acid (Asn481) is present in SARS-CoV-2 loop. The absence of two Pro residues, presence of Gly and Cys, and insertion of Asn481 in SARS-CoV-2 make the capping loop more flexible (RMSF∼0.8 nm) (Figure 3(B)). However, interface residues showed overall low RMSF (0.1–0.2 nm) and all critical amino acids maintain their interactions with ΔABP-α2 peptide. The single α helical peptide inhibitor of SARS-CoV-2 based on PD domain of hACE2 was found to be less stable (Han & Král, 2020). However, ΔABP-α2 peptide retains its shape and provides full coverage to RBM site (Figure 3(B)).

Radius of gyration (Rg) is the measure the compactness of the molecule in the solution. The Rg of SARS-CoV-2 RBD/ΔABP-α2 complex fluctuates between 1.87 and 1.97 nm. Significant variation is seen at around 50 ns simulation which can be attributed to the flexible loops of RBD (Figure 3(C)). Similarly, solvent accessible surface area (SASA) curve supports the Rg plot (Figure 3(D)). Thus, classical MD simulation studies suggest that the interface of the complex is stable, and the inhibitor ΔABP-α2 does not dissociate from RBD. A

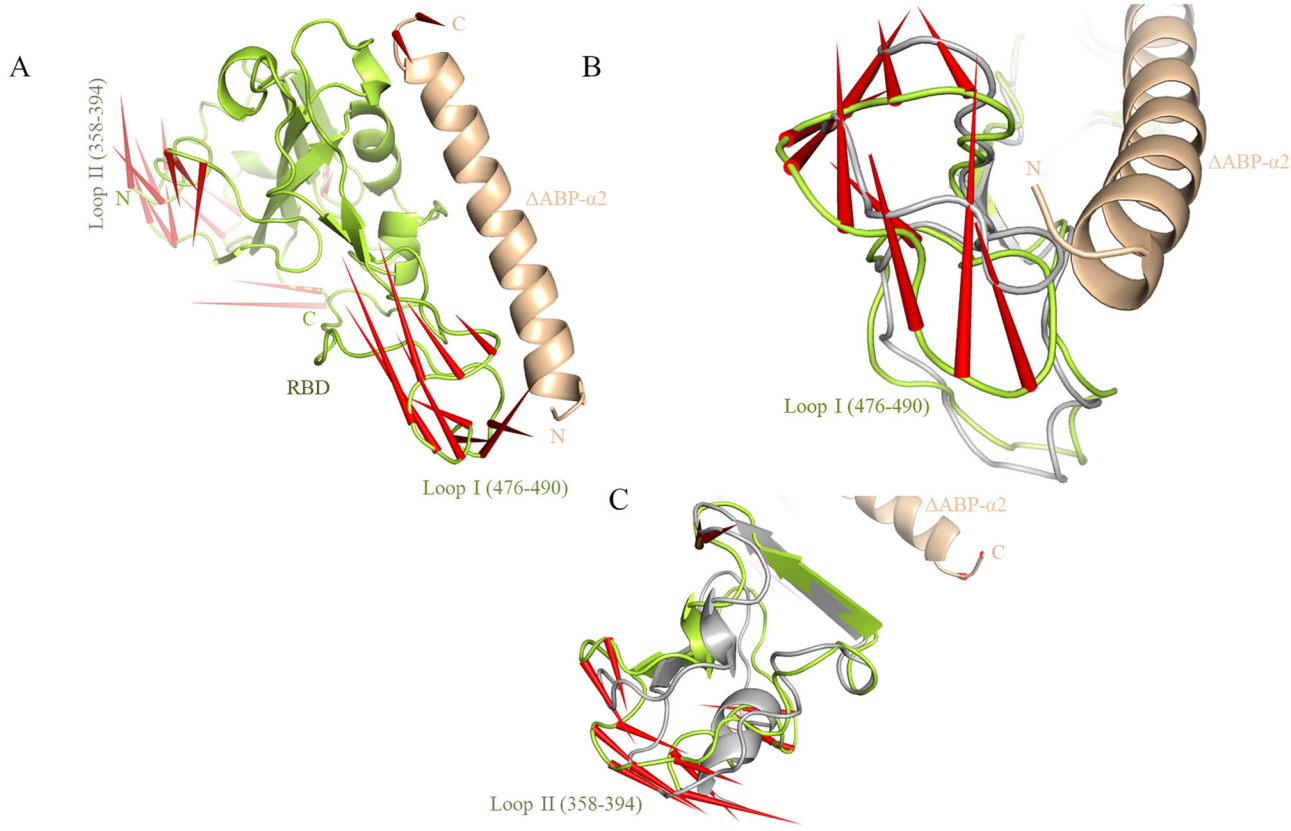

Figure 4. Dominant motion of SARS-CoV-2/ΔABP-α2 complex using principal component analysis. (A) Porcupine plot of the first eigenvector of SARS-CoV-2/ΔABP-α2 complex. (B) The capping loop I (476–490) near RBM site and C) loop II (358-394) show the maximum motion. SARS-CoV-2 RBD and ΔABP-α2 are shown in limon and wheat colour, respectively. Last frame of RBD is shown in grey.

good peptide inhibitor should have selective binding to the receptor, complementary shape and low flexibility of the interface residues (Wójcik & Berlicki, 2016).

Principle component analysis (PCA)

PCA is a standard method to characterise the variable correlations from atomic fluctuations in an MD trajectory. PCA can provide a brief description of the motions. PCA extracts highly correlated motions from the MD trajectories using dimensional reductions. To understand the motion of ΔABP-α2 peptide, RBM site and capping loop, PCA analysis was performed (Figure 4). The core of the RBD, the bound peptide and RBM site do not show any motion (Figure 4(A)). The C terminus of peptide showed slight twisting motion and shifted away from RBD significantly (∼6.0 Å). However, these residues are not involved in the direct interaction with RBD. Without complete protein fold, isolated helical peptides are usually unstable which in turn reduces the affinity of the peptides to the target protein (Chakrabartty et al., 1994). The peptide ΔABP-α2 maintained its helicity and remained bound to viral RBD throughout the simulations. The pose of peptide did not change during the simulation. Specially, the central portion of peptide ΔABP-α2 maintained its interaction with viral RBD (Supplementary File 2).

However, the capping loop (476–490) of RBD showed the highest degree of motion (Figure 4(B)). The capping loop fluctuates between open and close conformations (Figure 4(B) and Supplementary File 2). The ΔABP-α2 peptide maintains its interaction with capping loop throughout its transition from open to closed state. The second significant motion occurred in the fragment between residues (358–394) of RBD. This region is on the surface of RBD and far from the interface of RDM and ΔABP-α2 peptide (Figure 4(C)).

Immunoinformatics

The peptide inhibitor is recognised as a foreign substance by the human host cells, thus inducing a host immune response (Fernandez et al., 2018). The antibodies can affect the efficacy of the drug by reducing the lifetime, neutralising the activity and altering the pharmacokinetics of the drug. Thus, an ideal inhibitor should not be antigenic. The ΔABP-α2 peptide was not antigenic according to VaxiJen version 2.0 server (Doytchinova & Flower, 2007). The server predicted protective antigen score of −0.0046, which is much lower than the threshold 0.4. The B cell epitope is a portion of an antigen recognised by either a particular B cell receptor or the elicited antibody (Parker, 2016). There are two types of B cell epitopes – (1) Continuous and linear and (2) Discontinuous or structural. More than 90% of B cell epitopes are structural (El-Manzalawy & Honavar, 2010; Potocnakova et al., 2016; Sanchez-Trincado et al., 2017). DiscoTope analysis suggests the propensity scores of the individual residues for discontinuous B cell epitope (Figure 5(A)). The server did not find any B cell epitope on ΔABP-α2 surface.

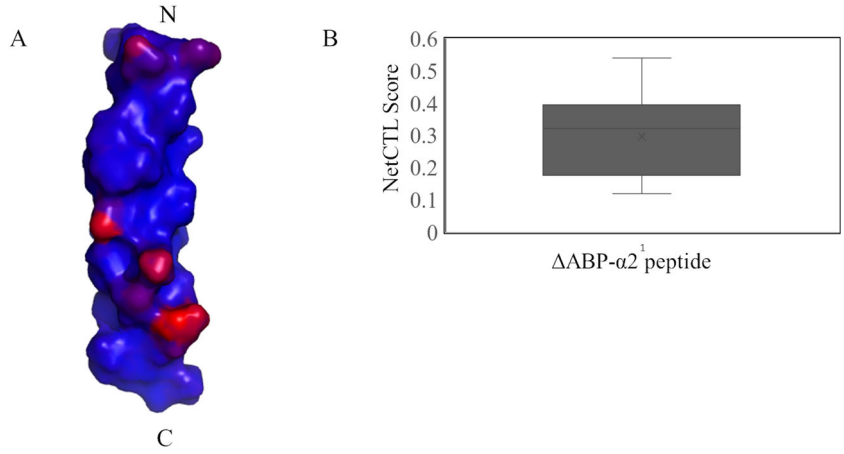

Figure 5. Immunoinformatics analysis of ΔABP-α2 peptide. (A) DiscoTope analysis predicted the propensity score of B cell epitope. The residues shown in red are potential B cell epitope. (B) Box plot depicting NetCTL scores for predictions of cytotoxic T lymphocyte (CTL) epitopes on the ΔABP-α2 peptide.

The recognition of viral peptides-MHC class I complex by CD8+ T cells is necessary for antiviral immunity. The T cell epitopes are necessary to design an effective vaccine, however, will pose a challenge to peptide-based drugs. We used NetCTL version 1.2 server to predict Cytotoxic T lymphocyte (CTL) epitopes (Figure 5(B)). This tool outcomes combined score of MHC class I binding, proteasomal C terminal cleavage and TAP transport efficiency. The highest score (0.5391) was predicted for peptide (LVENNRLNV) fragment. Thus, no CTL epitopes were predicted on ΔABP-α2 sequence. ToxinPred is an *in-silico* method to predict the toxicity of a peptide. The server uses a support vector machine (SVM) to predict toxicity along with all possible mutations (Gupta et al., 2013). The server predicted the toxic score of −0.90 with the threshold 0.1 used for calculation. Thus, immunoinformatics analysis suggests that ΔABP-α2 is non-immunogenic and non-toxic peptide. Therefore, it will be a probable candidate for therapeutic use.

Discussion

The COVID-19 pandemic has caused the inconceivable loss to the economy and human lives. The vaccines have been proved to be the most powerful tool to fight the viral infections. However, traditional drug discovery is not an efficient option as it takes longer time. Different strategies have been employed to develop therapeutics to combat the SARS-CoV-2 (Alattar et al., 2020; Dong et al., 2020; Thanh Le et al., 2020; Wu, Liu, et al., 2020; Zhou et al., 2006). The molecules that can effectively check the interaction of SARS-CoV-2 S protein with hACE2 will be a potential drug candidate. Here, we have reported a potential peptide ΔABP-α2 to block the association of S protein with hACE2. Thus, this study addresses an important problem to combat COVID-19. Computer aided drug design has become an indispensable too in drug discovery. We have proposed a lead inhibitor using computational approach to block the association of coronavirus to human host. The proposed study paves the path for synthesis, screening and validation of proposed inhibitor on biological system.

Peptides are smaller and easy to produce either chemically or biologically. The advantages of peptides as drugs include the low toxicity, ease of modifications, specificity to the target, greater affinity, etc. Peptide inhibitors have been reported to block the SARS-CoV-2 attachment to hACE2. These peptide inhibitors are derived either from the interaction site of RBD/hACE2 or *de novo* designed to bind viral RBD. Some peptide inhibitors are also reported to bind non-interface region of S protein. Huang et al. have proposed a peptide inhibitor for SARS-CoV-2/hACE2 association using EvoDesign approach (Huang et al., 2020). The proposed inhibitor showed a stronger binding affinity to RBD compared to hACE2 (Huang et al., 2020). Hsiang et al. have shown that the peptides SP-4 (GFLYV YKGYQPI), SP-8 (FYTTTGIGYQPY) and SP-10 (STSQKSIVAYTM) can significantly block the interaction of SARS-CoV S protein with hACE2 (Ho et al., 2006). However, these peptides are derived from viral spike protein and their target is hACE2. This will limit their use as therapeutics because they might affect normal function of hACE2 (Ho et al., 2006). Alanine scanning showed that residues between 22 and 57 of hACE2 are important for its binding with viral RBD. Several peptide inhibitors have been reported based on this region of hACE2 (Baig et al., 2020; D. P. Han et al., 2006). Han and Kral (2020) also showed potential peptide inhibitors of RBD derived from PD domain of hACE2. Similarly, Barh et al. have designed several peptides with potential to block the association of SARS-CoV-2 RBD and hACE2 (Potential chimeric peptides to block the SARS-CoV-2 Spike RBD). Miniproteins AHB1 and AHB2 were designed using ACE2 as scaffold. They neutralised SARS-CoV-2 with IC50 35 and 16 nM, respectively. Employing de novo approach, two mini proteins LCB1 and LCB3 were identified. The LCB1 and LCB3 neutralised SARS-CoV-2 in picomolar range. These miniproteins showed cross reactivity with SARS-CoV RBD (Cao et al., 2020). Similarly, a 23 mer peptide fragment derived from α1/ACE2 helix was reported to bind specifically SARS-CoV-2 RBD with nanomolar affinity (Zhang et al., 2020). Thus, RBD is suitable target for virus inhibition. Peptide inhibitors derived from PD domain of hACE2 has the potential to block the association of coronavirus to host cell.

One critical limitation in using peptide inhibitors as drug is their short half-life *in vivo*. However, the conjugation of

peptides with lipid exhibit significantly improved antiviral potency and better pharmacokinetics (Chong et al., 2017; Vilas Boas et al., 2019). The field of peptidomimetics is used to get derivatives of peptides which have better bioavailability, improved blood-brain barrier transport, reduced rate of clearance and better stability against peptidases (Lenci & Trabocchi, 2020; Vagner et al., 2008). Some examples of peptidomimetics are the D-amino acid substitutes, altered amide bonds, peptoids, urea peptidomimetics, peptide sulfonamides, oligocarbamates, partial or full retro-inverso peptides, azapeptides, β-peptides and N-modified peptides etc. Further, computational protein design can be combined with experimental setup to accelerate the drug design. We have verified the binding of ΔABP-α2 peptide to SARS-CoV-2 RBD by various computational tools. However, it warrants the experimental verification to assess the drug ability of ΔABP-α2.

Conclusion

In summary, using classical MD simulations, we have shown that the peptide ΔABP-α2 extracted from ABP provide a highly promising trail for SARS-CoV-2 blocking. MD simulations revealed that the peptides maintain their helical structure and provide a highly specific and stable binding to SARS-CoV-2 RBD. The ΔABP-α2 peptide specifically engages with critical residues of SARS-CoV-2 RBD. Binding affinity prediction suggests that the peptide binds to viral RBD with ∼95-fold higher affinity than hACE2. Thus, the peptide will outcompete the hACE2. Immunoinformatics analysis suggests that proposed peptide inhibitor is non-immunogenic and nontoxic.

Acknowledgements

We would like to acknowledge the Ramalingaswami Fellowship (BT/RLF/Re-entry/64/2017), Department of Biotechnology, Govt of India (VK). The funders had no role in study design, data collection and analysis, decision to publish or preparation of the manuscript.

Author contribution

Conceived and designed the experiments: VK. Performed the experiments: GJ, SY and VK. Analysed the data: GJ, SY and VK. Contributed to the writing of the manuscript: VK.

Disclosure statement

The authors declare no competing financial interest.

Funding

This work was supported by Department of Biotechnology, Ministry of Science and Technology.

ORCID

Veerendra Kumar http://orcid.org/0000-0002-9241-1303

References

Abraham, M. J., Murtola, T., Schulz, R., Páll, S., Smith, J. C., Hess, B., & Lindah, E. (2015). Gromacs: High performance molecular simulations through multi-level parallelism from laptops to supercomputers. *SoftwareX*, *1–2*, 19–25. https://doi.org/10.1016/j.softx.2015.06.001

Alattar, R., Ibrahim, T. B. H., Shaar, S. H., Abdalla, S., Shukri, K., Daghfal, J. N., Khatib, M. Y., Aboukamar, M., Abukhattab, M., Alsoub, H. A., Almaslamani, M. A., & Omrani, A. S. (2020). Tocilizumab for the treatment of severe coronavirus disease 2019. *Journal of Medical Virology*, *92*(10), 2042–2049. https://doi.org/10.1002/jmv.25964

Ali, A., & Vijayan, R. (2020). Dynamics of the ACE2–SARS-CoV-2/SARS-CoV spike protein interface reveal unique mechanisms. *Scientific Reports*, *10*(1), 14214. https://doi.org/10.1038/s41598-020-71188-3

Baig, M. S., Alagumuthu, M., Rajpoot, S., & Saqib, U. (2020). Identification of a potential peptide inhibitor of SARS-CoV-2 targeting its entry into the host cells. *Drugs in R and D*, *20*(3), 161–169. https://doi.org/10.1007/s40268-020-00312-5

Belouzard, S., Millet, J. K., Licitra, B. N., & Whittaker, G. R. (2012). Mechanisms of coronavirus cell entry mediated by the viral spike protein. *Viruses*, *4*(6), 1011–1033. https://doi.org/10.3390/v4061011

Berman, H. M., Westbrook, J., Feng, Z., Gilliland, G., Bhat, T. N., Weissig, H., Shindyalov, I. N., & Bourne, P. E. (2000). The protein data bank (www.rcsb.org). *Nucleic Acids Research*, *28*(1), 235–242. https://doi.org/10.1093/nar/28.1.235

Bosch, B. J., van der Zee, R., de Haan, C. A. M., & Rottier, P. J. M. (2003). The coronavirus spike protein is a class I virus fusion protein: structural and functional characterization of the fusion core complex. *Journal of Virology*, *77*(16), 8801–8811. https://doi.org/10.1128/JVI.77.16.8801-8811.2003

Brandman, R., Brandman, Y., & Pande, V. S. (2012). A-site residues move independently from P-site residues in all-atom molecular dynamics simulations of the 70S bacterial ribosome. *PLoS One*, *7*(1), e29377. https://doi.org/10.1371/journal.pone.0029377

Cao, L., Goreshnik, I., Coventry, B., Case, J. B., Miller, L., Kozodoy, L., Chen, R. E., Carter, L., Walls, A. C., Park, Y. J., Strauch, E. M., Stewart, L., Diamond, M. S., Veesler, D., & Baker, D. (2020). De novo design of picomolar SARS-CoV-2 miniprotein inhibitors. *Science*, *370*(6515), 426–431. https://doi.org/10.1126/science.abd9909

Casalino, L., Gaieb, Z., Goldsmith, J. A., Hjorth, C. K., Dommer, A. C., Harbison, A. M., Fogarty, C. A., Barros, E. P., Taylor, B. C., Mclellan, J. S., Fadda, E., & Amaro, R. E. (2020). Beyond shielding: The roles of glycans in the SARS-CoV-2 spike protein. *ACS Central Science*, *6*(10), 1722–1734. https://doi.org/10.1021/acscentsci.0c01056

Chakrabartty, A., Kortemme, T., & Baldwin, R. L. (1994). Helix propensities of the amino acids measured in alanine-based peptides without helix-stabilizing side-chain interactions. *Protein Science: A Publication of the Protein Society*, *3*(5), 843–852. https://doi.org/10.1002/pro.5560030514

Chandel, V., Raj, S., Rathi, B., & Kumar, D. (2020). In silico identification of potent FDA approved drugs against coronavirus COVID-19 main protease: A drug repurposing approach. *Chemical Biology Letters*, *7*, 2347–9825. http://www.pubs.iscience.in/journal/index.php/cbl/article/view/1033/0

Chong, H., Xue, J., Xiong, S., Cong, Z., Ding, X., Zhu, Y., Liu, Z., Chen, T., Feng, Y., He, L., Guo, Y., Wei, Q., Zhou, Y., Qin, C., & He, Y. (2017). A lipopeptide HIV-1/2 fusion inhibitor with highly potent in vitro, ex vivo, and in vivo antiviral activity. *Journal of Virology*, *91*(11), 1–13. https://doi.org/10.1128/JVI.00288-17

Coutard, B., Valle, C., de Lamballerie, X., Canard, B., Seidah, N. G., & Decroly, E. (2020). The spike glycoprotein of the new coronavirus 2019-nCoV contains a furin-like cleavage site absent in CoV of the same clade. *Antiviral Research*, *176*, 104742. https://doi.org/10.1016/j.antiviral.2020.104742

de Vries, S. J., & Bonvin, A. M. J. J. (2011). Cport: A consensus interface predictor and its performance in prediction-driven docking with HADDOCK. *PLoS One*, *6*(3), e17695. https://doi.org/10.1371/journal.pone.0017695

DeLano, W. L. (2002). *The PyMOL molecular graphics system, version 1.1. Schr{ö}dinger LLC*, https://doi.org/10.1038/hr.2014.17

Dong, L., Hu, S., & Gao, J. (2020). Discovering drugs to treat coronavirus disease 2019 (COVID-19. *Drug Discoveries & Therapeutics*, *14*(1), 58–60. https://doi.org/10.5582/ddt.2020.01012

Doytchinova, I. A., & Flower, D. R. (2007). VaxiJen: A server for prediction of protective antigens, tumour antigens and subunit vaccines. *BMC Bioinformatics*, *8*(1), 1–7. https://doi.org/10.1186/1471-2105-8-4

El-Manzalawy, Y., & Honavar, V. (2010). Recent advances in B-cell epitope prediction methods. *Immunome Research*, *6*(2), 1–9. https://doi.org/10.1186/1745-7580-6-S2-S2

Emsley, P., Lohkamp, B., Scott, W. G., & Cowtan, K. (2010). Features and development of Coot. *Acta Crystallographica Section D: Biological Crystallography*, *66*(6), 486–501. https://doi.org/10.1107/S0907444910007493

Feldmann, M., Maini, R. N., Woody, J. N., Holgate, S. T., Winter, G., Rowland, M., Richards, D., & Hussell, T. (2020). Trials of anti-tumour necrosis factor therapy for COVID-19 are urgently needed. *The Lancet*, *395*(10234), 1407–1409. https://doi.org/10.1016/S0140-6736(20)30858-8

Fernandez, L., Bustos, R. H., Zapata, C., Garcia, J., Jauregui, E., & Ashraf, G. M. (2018). Immunogenicity in protein and peptide based-therapeutics: An overview. *Current Protein & Peptide Science*, *19*(10), 958–971. https://doi.org/10.2174/1389203718666170828123449

Gao, J., Lu, G., Qi, J., Li, Y., Wu, Y., Deng, Y., Geng, H., Li, H., Wang, Q., Xiao, H., Tan, W., Yan, J., & Gao, G. F. (2013). Structure of the fusion core and inhibition of fusion by a heptad repeat peptide derived from the S protein of middle east respiratory syndrome coronavirus. *Journal of Virology*, *87*(24), 13134–13140. https://doi.org/10.1128/JVI.02433-13

Gupta, S., Kapoor, P., Chaudhary, K., Gautam, A., Kumar, R., & Raghava, G. P. S, Open Source Drug Discovery Consortium (2013). In silico approach for predicting toxicity of peptides and proteins. *PLoS One*, *8*(9), e73957. https://doi.org/10.1371/journal.pone.0073957

Han, D. P., Penn-Nicholson, A., & Cho, M. W. (2006). Identification of critical determinants on ACE2 for SARS-CoV entry and development of a potent entry inhibitor. *Virology*, *350*(1), 15–25. https://doi.org/10.1016/j.virol.2006.01.029

Han, Y., & Král, P. (2020). Computational design of ACE2-based peptide inhibitors of SARS-CoV-2. *ACS Nano*, *14*(4), 5143–5147. https://doi.org/10.1021/acsnano.0c02857

Ho, T. Y., Wu, S. L., Chen, J. C., Wei, Y. C., Cheng, S. E., Chang, Y. H., Liu, H. J., & Hsiang, C. Y. (2006). Design and biological activities of novel inhibitory peptides for SARS-CoV spike protein and angiotensin-converting enzyme 2 interaction. *Antiviral Research*, *69*(2), 70–76. https://doi.org/10.1016/j.antiviral.2005.10.005

Hoffmann, M., Kleine-Weber, H., & Pöhlmann, S. (2020). A multibasic cleavage site in the spike protein of SARS-CoV-2 is essential for infection of human lung cells. *Molecular Cell*, *78*(4), 779–784. https://doi.org/10.1016/j.molcel.2020.04.022

Huang, X., Pearce, R., & Zhang, Y. (2020). De novo design of protein peptides to block association of the SARS-CoV-2 spike protein with human ACE2. *Aging*, *12*(12), 11263–11276. https://doi.org/10.18632/aging.103416

Jaiswal, G., & Kumar, V. (2020). In-silico design of a potential inhibitor of SARS-CoV-2 S protein. *PLOS One*, *15*(10), e0240004. https://doi.org/10.1371/journal.pone.0240004

Jo, S., Kim, T., Iyer, V. G., & Im, W. (2008). CHARMM-GUI: A web-based graphical user interface for CHARMM. *Journal of Computational Chemistry*, *29*(11), 1859–1865. https://doi.org/10.1002/jcc.20945

Khan, R. J., Jha, R. K., Amera, G. M., Jain, M., Singh, E., Pathak, A., Singh, R. P., Muthukumaran, J., & Singh, A. K. (2020). Targeting SARS-CoV-2: A systematic drug repurposing approach to identify promising inhibitors against 3C-like proteinase and 2′-O-ribosemethyltransferase. *Journal of Biomolecular Structure & Dynamics*, 1–14. https://doi.org/10.1080/07391102.2020.1753577

Kringelum, J. V., Lundegaard, C., Lund, O., & Nielsen, M. (2012). Reliable B cell epitope predictions: Impacts of method development and improved benchmarking. *PLoS Computational Biology*, *8*(12), e1002829. https://doi.org/10.1371/journal.pcbi.1002829

Kumar, S., Maurya, V. K., Prasad, A. K., Bhatt, M. L. B., & Saxena, S. K. (2020). Structural, glycosylation and antigenic variation between 2019 novel coronavirus (2019-nCoV) and SARS coronavirus (SARS-CoV. *Virusdisease*, *31*(1), 13–21. https://doi.org/10.1007/s13337-020-00571-5

Lan, J., Ge, J., Yu, J., Shan, S., Zhou, H., Fan, S., Zhang, Q., Shi, X., Wang, Q., Zhang, L., & Wang, X. (2020). Structure of the SARS-CoV-2 spike receptor-binding domain bound to the ACE2 receptor. *Nature*, *581*(7807), 215–220. https://doi.org/10.1038/s41586-020-2180-5

Larsen, M. v., Lundegaard, C., Lamberth, K., Buus, S., Lund, O., & Nielsen, M. (2007). Large-scale validation of methods for cytotoxic T-lymphocyte epitope prediction. *BMC Bioinformatics*, *8*(1), 424. https://doi.org/10.1186/1471-2105-8-424

Lee, J., Cheng, X., Swails, J. M., Yeom, M. S., Eastman, P. K., Lemkul, J. A., Wei, S., Buckner, J., Jeong, J. C., Qi, Y., Jo, S., Pande, V. S., Case, D. A., Brooks, C. L., MacKerell, A. D., Klauda, J. B., & Im, W. (2016). CHARMM-GUI input generator for NAMD, GROMACS, AMBER, openMM, and CHARMM/OpenMM simulations using the CHARMM36 additive force field. *Journal of Chemical Theory and Computation*, *12*(1), 405–413. https://doi.org/10.1021/acs.jctc.5b00935

Lenci, E., & Trabocchi, A. (2020). Peptidomimetic toolbox for drug discovery. *Chemical Society Reviews*, *49*(11), 3262–3277. https://doi.org/10.1039/D0CS00102C

Li, F. (2015). Receptor recognition mechanisms of coronaviruses: A decade of structural studies. *Journal of Virology*, *89*(4), 1954–1964. https://doi.org/10.1128/JVI.02615-14

Li, F. (2016). Structure, function, and evolution of coronavirus spike proteins. *Annual Review of Virology*, *3*(1), 237–261. https://doi.org/10.1146/annurev-virology-110615-042301

Li, F., Li, W., Farzan, M., & Harrison, S. C. (2005). Structural biology: Structure of SARS coronavirus spike receptor-binding domain complexed with receptor. *Science*, *309*(5742), 1864–1868. https://doi.org/10.1126/science.1116480

Li, W., Greenough, T. C., Moore, M. J., Vasilieva, N., Somasundaran, M., Sullivan, J. L., Farzan, M., & Choe, H. (2004). Efficient replication of severe acute respiratory syndrome coronavirus in mouse cells is limited by murine angiotensin-converting enzyme 2. *Journal of Virology*, *78*(20), 11429–11433. https://doi.org/10.1128/JVI.78.20.11429-11433.2004

Li, W., Moore, M. J., Vasilieva, N., Sui, J., Wong, S. K., Berne, M. A., Somasundaran, M., Sullivan, J. L., Luzuriaga, K., Greenough, T. C., Choe, H., & Farzan, M. (2003). Angiotensin-converting enzyme 2 is a functional receptor for the SARS coronavirus. *Nature*. *Nature*, *426*(6965), 450–454. https://doi.org/10.1038/nature02145

Mirza, M. U., & Froeyen, M. (2020). Structural elucidation of SARS-CoV-2 vital proteins: Computational methods reveal potential drug candidates against main protease, Nsp12 RNA-dependent RNA polymerase and Nsp13 helicase. *Journal of pharmaceutical analysis*, *10*(4), 320–328. https://doi.org/10.20944/preprints202003.0085.v1

Parker, D. C. (2016). T cell-dependent B cell activation. *Encyclopedia of Immunobiology*. https://doi.org/10.1016/B978-0-12-374279-7.09010-X

Pettersen, E. F., Goddard, T. D., Huang, C. C., Couch, G. S., Greenblatt, D. M., Meng, E. C., & Ferrin, T. E. (2004). UCSF Chimera-a visualization system for exploratory research and analysis. *Journal of Computational Chemistry*, *25*(13), 1605–1612. https://doi.org/10.1002/jcc.20084

Potocnakova, L., Bhide, M., & Pulzova, L. B. (2016). An introduction to B-cell epitope mapping and in silico epitope prediction. *Journal of Immunology Research*, *2016*, 6760830. https://doi.org/10.1155/2016/6760830

Rath, S. L., & Kumar, K. (2020). Investigation of the effect of temperature on the structure of SARS-CoV-2 spike protein by molecular dynamics aimulations. *Frontiers in Molecular Biosciences*, *7*, 583523. https://doi.org/10.3389/fmolb.2020.583523

Ren, L. L., Wang, Y. M., Wu, Z. Q., Xiang, Z. C., Guo, L., Xu, T., Jiang, Y. Z., Xiong, Y., Li, Y. J., Li, X. W., Li, H., Fan, G. H., Gu, X. Y., Xiao, Y., Gao, H., Xu, J. Y., Yang, F., Wang, X. M., Wu, C., … Wang, J. W. (2020). Identification of a novel coronavirus causing severe pneumonia in human: A descriptive study. *Chinese Medical Journal*, *133*(9), 1015–1024. https://doi.org/10.1097/CM9.0000000000000722

Roccatano, D., Barthel, A., & Zacharias, M. (2007). Structural flexibility of the nucleosome core particle at atomic resolution studied by molecular dynamics simulation. *Biopolymers*, *85*(5–6), 407–421. https://doi.org/10.1002/bip.20690

Sanchez-Garcia, R., Sorzano, C. O. S., Carazo, J. M., & Segura, J. (2019). BIPSPI: A method for the prediction of partner-specific protein-protein interfaces. *Bioinformatics*, *35*(3), 470–477. https://doi.org/10.1093/bioinformatics/bty647

Sanchez-Trincado, J. L., Gomez-Perosanz, M., & Reche, P. A. (2017). Fundamentals and methods for T- and B-cell epitope prediction. *Journal of Immunology Research*, *2017*, 2680160. https://doi.org/10.1155/2017/2680160

Shang, J., Ye, G., Shi, K., Wan, Y., Luo, C., Aihara, H., Geng, Q., Auerbach, A., & Li, F. (2020). Structural basis of receptor recognition by SARS-CoV-2. *Nature*, *581*(7807), 221–224. https://doi.org/10.1038/s41586-020-2179-y

Sharma, S., Ding, F., & Dokholyan, N. v. (2007). Multiscale modeling of nucleosome dynamics. *Biophysical Journal*, *92*(5), 1457–1470. https://doi.org/10.1529/biophysj.106.094805

Simmons, G., Reeves, J. D., Rennekamp, A. J., Amberg, S. M., Piefer, A. J., & Bates, P. (2004). Characterization of severe acute respiratory syndrome-associated coronavirus (SARS-CoV) spike glycoprotein-mediated viral entry. *Proceedings of the National Academy of Sciences of the United States of America*, *101*(12), 4240–4245. https://doi.org/10.1073/pnas.0306446101

Spaan, W., Cavanagh, D., & Horzinek, M. C. (1988). Coronaviruses: Structure and genome expression. *Journal of General Virology*, *69*(12), 2939–2952. https://doi.org/10.1099/0022-1317-69-12-2939

Tai, W., He, L., Zhang, X., Pu, J., Voronin, D., Jiang, S., Zhou, Y., & Du, L. (2020). Characterization of the receptor-binding domain (RBD) of 2019 novel coronavirus: Implication for development of RBD protein as a viral attachment inhibitor and vaccine. *Cellular and Molecular Immunology*, *17*(6), 613–620. https://doi.org/10.1038/s41423-020-0400-4

Thanh Le, T., Andreadakis, Z., Kumar, A., Gómez Román, R., Tollefsen, S., Saville, M., & Mayhew, S. (2020). The COVID-19 vaccine development landscape. *Nature reviews Drug discovery*, *19*(5), 305–306. https://doi.org/10.1038/d41573-020-00073-5

Tian, X., Li, C., Huang, A., Xia, S., Lu, S., Shi, Z., Lu, L., Jiang, S., Yang, Z., Wu, Y., & Ying, T. (2020). Potent binding of 2019 novel coronavirus spike protein by a SARS coronavirus-specific human monoclonal antibody. *Emerging Microbes and Infections*, *9*(1), 382–385. https://doi.org/10.1080/22221751.2020.1729069

Tinoco, I., & J. der, W. (2009). Simulation and analysis of single-ribosome translation. *Physical Biology*, *6*(2), 025006. https://doi.org/10.1088/1478-3975/6/2/025006

Vagner, J., Qu, H., & Hruby, V. J. (2008). Peptidomimetics, a synthetic tool of drug discovery. *Current Opinion in Chemical Biology*, *12*(3), 292–296. https://doi.org/10.1016/j.cbpa.2008.03.009

van Zundert, G. C. P., Rodrigues, J. P. G. L. M., Trellet, M., Schmitz, C., Kastritis, P. L., Karaca, E., Melquiond, A. S. J., van Dijk, M., de Vries, S. J., & Bonvin, A. M. J. J. (2016). The HADDOCK2.2 web server: User-friendly integrative modeling of biomolecular complexes. *Journal of Molecular Biology*, *428*(4), 720–725. https://doi.org/10.1016/j.jmb.2015.09.014

Vilas Boas, L. C. P., Campos, M. L., Berlanda, R. L. A., de Carvalho Neves, N., & Franco, O. L. (2019). Antiviral peptides as promising therapeutic drugs. *Cellular and Molecular Life Sciences*, *76*(18), 3525–3542. https://doi.org/10.1007/s00018-019-03138-w

Walls, A. C., Park, Y. J., Tortorici, M. A., Wall, A., McGuire, A. T., & Veesler, D. (2020). Structure, Function, and Antigenicity of the SARS-CoV-2 Spike Glycoprotein. *Cell*, *181*(2), 281–292. https://doi.org/10.1016/j.cell.2020.02.058

Walls, A. C., Tortorici, M. A., Frenz, B., Snijder, J., Li, W., Rey, F. A., DiMaio, F., Bosch, B. J., & Veesler, D. (2016). Glycan shield and epitope masking of a coronavirus spike protein observed by cryo-electron microscopy. *Nature Structural and Molecular Biology*, 23(10), 899–905. https://doi.org/10.1038/nsmb.3293

Wan, Y., Shang, J., Graham, R., Baric, R. S., & Li, F. (2020). Receptor recognition by the novel coronavirus from Wuhan: An analysis based on decade-long structural studies of SARS coronavirus. *Journal of Virology*, *94*(7), e00127–20. https://doi.org/10.1128/JVI.00127-20

Weng, G., Wang, E., Wang, Z., Liu, H., Zhu, F., Li, D., & Hou, T. (2019). HawkDock: A web server to predict and analyze the protein-protein complex based on computational docking and MM/GBSA. *Nucleic Acids Research*, *47*(W1), W322–W330. https://doi.org/10.1093/nar/gkz397

Wójcik, P., & Berlicki, Ł. (2016). Peptide-based inhibitors of protein–protein interactions. *Bioorganic and Medicinal Chemistry Letters*, *26*(3):707–713. https://doi.org/10.1016/j.bmcl.2015.12.084

Wrapp, D., Wang, N., Corbett, K. S., Goldsmith, J. A., Hsieh, C. L., Abiona, O., Graham, B. S., & McLellan, J. S. (2020). Cryo-EM structure of the 2019-nCoV spike in the prefusion conformation. *Science*, *367*(6483), 1260–1263. https://doi.org/10.1126/science.aax0902 https://doi.org/10.1126/science.abb2507

Wu, C., Liu, Y., Yang, Y., Zhang, P., Zhong, W., Wang, Y., Wang, Q., Xu, Y., Li, M., Li, X., Zheng, M., Chen, L., & Li, H. (2020). Analysis of therapeutic targets for SARS-CoV-2 and discovery of potential drugs by computational methods. *Acta Pharmaceutica Sinica. B*, *10*(5), 766–788. https://doi.org/10.1016/j.apsb.2020.02.008

Wu, F., Zhao, S., Yu, B., Chen, Y. M., Wang, W., Song, Z. G., Hu, Y., Tao, Z. W., Tian, J. H., Pei, Y. Y., Yuan, M. L., Zhang, Y. L., Dai, F. H., Liu, Y., Wang, Q. M., Zheng, J. J., Xu, L., Holmes, E. C., & Zhang, Y. Z. (2020). A new coronavirus associated with human respiratory disease in China. *Nature*, *579*(7798), 265–269. https://doi.org/10.1038/s41586-020-2008-3

Xia, S., Zhu, Y., Liu, M., Lan, Q., Xu, W., Wu, Y., Ying, T., Liu, S., Shi, Z., Jiang, S., & Lu, L. (2020). Fusion mechanism of 2019-nCoV and fusion inhibitors targeting HR1 domain in spike protein. *Cellular and Molecular Immunology*, *17*(7):765–767 https://doi.org/10.1038/s41423-020-0374-2

Xue, L. C., Rodrigues, J. P., Kastritis, P. L., Bonvin, A. M., & Vangone, A. (2016). PRODIGY: A web server for predicting the binding affinity of protein–protein complexes. *Bioinformatics*, *32*(23):3676–3678. https://doi.org/10.1093/bioinformatics/btw514

Yan, R., Zhang, Y., Li, Y., Xia, L., Guo, Y., & Zhou, Q. (2020). Structural basis for the recognition of SARS-CoV-2 by full-length human ACE2. *Science*, *367*(6485), 1444–1448. https://doi.org/10.1126/science.abb2762

Yang, L. W., Eyal, E., Bahar, I., & Kitao, A. (2009). Principal component analysis of native ensembles of biomolecular structures (PCA_NEST): Insights into functional dynamics. *Bioinformatics*, *25*(5), 606–614. https://doi.org/10.1093/bioinformatics/btp023

Zhang, G., Pomplun, S., Loftis, A. R., Tan, X., Loas, A., & Pentelute, B. L. (2020). Investigation of ACE2 N-terminal fragments binding to SARS-CoV-2 Spike RBD. *BioRxiv*.

Zhou, P., Yang, X. L., Wang, X. G., Hu, B., Zhang, L., Zhang, W., Si, H. R., Zhu, Y., Li, B., Huang, C. L., Chen, H.D., Chen, J., Luo, Y., Guo, H., Jiang, R. D., Liu, M. Q., Chen, Y., Shen, X. R., Wang, X., & Shi, Z. L. (2020). A pneumonia outbreak associated with a new coronavirus of probable bat origin. *Nature*, *588*(7836), E6–E6. https://doi.org/10.1038/s41586-020-2012-7

Zhou, Y., Hou, Y., Shen, J., Huang, Y., Martin, W., & Cheng, F. (2020). Network-based drug repurposing for novel coronavirus 2019-nCoV/SARS-CoV-2. *Cell Discovery*, *6*(1):14. https://doi.org/10.1038/s41421-020-0153-3

Zhou, Z., Post, P., Chubet, R., Holtz, K., McPherson, C., Petric, M., & Cox, M. (2006). A recombinant baculovirus-expressed S glycoprotein vaccine elicits high titers of SARS-associated coronavirus (SARS-CoV) neutralizing antibodies in mice. *Vaccine*, *24*(17), 3624–3631. https://doi.org/10.1016/j.vaccine.2006.01.059

Zhu, N., Zhang, D., Wang, W., Li, X., Yang, B., Song, J., Zhao, X., Huang, B., Shi, W., Lu, R., Niu, P., Zhan, F., Ma, X., Wang, D., Xu, W., Wu, G., Gao, G. F., & Tan, W, China Novel Coronavirus Investigating and Research Team. (2020). A novel coronavirus from patients with pneumonia in China, 2019. *The New England Journal of Medicine*, *382*(8), 727–733. https://doi.org/10.1056/NEJMoa2001017